A&A 620, A34 (2018)
https://doi.org/10.1051/0004-6361/201833330


Astronomy & Astrophysics

# HD 38858: a solar-type star with an activity cycle of ~10.8 yr

## Searching for variations in the Balmer and metallic lines⋆

M. Flores[1,3,5,⋆⋆], J. F. González[1,3,5], M. Jaque Arancibia[1,5,6], C. Saffe[1,3,5], A. Buccino[2,4,5], F. M. López[1,3,5], R. V. Ibañez Bustos[2,5], and P. Miquelarena[3]

[1] Instituto de Ciencias Astronómicas, de la Tierra y del Espacio (ICATE), España Sur 1512, CC 49, 5400 San Juan, Argentina
e-mail: matiasflorestrivigno@conicet.gov.ar
[2] Instituto de Astronomía y Física del Espacio (IAFE), Buenos Aires, Argentina
e-mail: jfgonzalez@conicet.gov.ar
[3] Facultad de Ciencias Exactas, Físicas y Naturales, Universidad Nacional de San Juan, San Juan, Argentina
e-mail: mjaque@conicet.gov.ar
[4] Departamento de Física, Facultad de Ciencias Exactas y Naturales, Universidad de Buenos Aires, Buenos Aires, Argentina
[5] Consejo Nacional de Investigaciones Científicas y Técnicas (CONICET), Argentina
[6] Departamento de Física y Astronomía, Universidad de La Serena, Av. Cisternas 1200, La Serena, Chile

Received 30 April 2018 / Accepted 13 September 2018

**ABSTRACT**

*Context.* The detection of chromospheric activity cycles in solar-analogue and twin stars can be used to place the solar cycle in a wider context. However, relatively few of these stars with activity cycles have been detected. It is well known that the cores of the Ca II H&K lines are modulated by stellar activity. The behaviour of the Balmer and other optical lines with stellar activity is not yet completely understood.
*Aims.* We search for variations in the Ca II H&K, Balmer, and Fe II lines modulated by stellar activity. In particular, we apply a novel strategy to detect possible shape variations in the H$\alpha$ line.
*Methods.* We analysed activity signatures in HD 38858 using HARPS and CASLEO spectra obtained between 2003 and 2017. We calculated the Mount Wilson index ($S_{\rm MW}$), $\log(R'_{\rm HK})$, and the statistical moments of the Ca II H&K, Balmer, and other optical lines. We searched for periodicities using the generalized Lomb-Scargle periodogram.
*Results.* We detect a long-term activity cycle of 10.8 yr in Ca II H&K and H$\alpha$ in the solar-analogue star HD 38858. In contrast, this cycle is marginally detected in the Fe II lines. We also detect a noticeable variation in radial velocity that seems to be produced by stellar activity.
*Conclusions.* HD 38858 is the second solar-analogue star where we find a clear activity cycle that is replicated in the Balmer lines. Spectral indexes based on the shape of H$\alpha$ line seem to be more reliable than the fluxes in the same line for detecting activity variations. The cyclic modulation we detected gives place to a variation in radial velocity that previously has been associated with a super-Earth planet. Finally, due to the similarity of HD 38858 with the Sun, we recommend to continue monitoring this star.

**Key words.** stars: activity – stars: chromospheres – stars: solar-type – stars: individual: HD 38858

## 1. Introduction

Wilson (1978) showed for the first time that solar-type stars might show long-term chromospheric variations in their Ca II H&K lines. This was followed by several studies, mainly the HK project at the Mount Wilson Observatory (e.g. Vaughan et al. 1978; Duncan et al. 1991; Baliunas et al. 1995; Henry et al. 1996). Different works also showed that stellar activity is related to important variables such as rotation, differential rotation, and the stellar age (e.g. Skumanich 1972; Donahue 1993; Mamajek & Hillenbrand 2008). These studies established the basis of the current knowledge of activity for stars in the solar neighborhood.

Activity studies of stars that are physically similar to our Sun deserve particular attention because they help us to place its ~11 yr cycle in context. For instance, the solar-twin star 18 Sco presents a cycle of 7.1 yr (Hall et al. 2007), while the solar-analogue HD 30495 shows short-period variations together with a long cycle of ~12 yr (Egeland et al. 2015). Both stars are younger than the Sun: 18 Sco is $3.8 \pm 0.5$ Gyr old (Nissen 2015) and HD 30495 is $0.97 \pm 0.12$ Gyr old (Egeland et al. 2015). In addition, we found a cycle of only ~5.1 yr in the solar-analogue HD 45184 (Flores et al. 2016), while in the $\zeta$ Ret binary system, the components simultaneously show erratic ($\zeta^1$ Ret) and cyclic activity patterns ($\zeta^2$ ~ 10 yr) (Flores et al. 2018); both stars are similar to the Sun (Saffe et al. 2016).

We have an ongoing programme that currently monitors the stellar activity in a sample of solar-analogue and solar-twin stars. For our studies, we mainly use the extensive data base of the High Accuracy Radial velocity Planet Searcher (HARPS)

⋆ Based on observations made with ESO Telescopes at the La Silla Paranal Observatory under programmes: 183.C-0972(A), 072.C-0488(E), 192.C-0852(A), 091.C-0936(A) and 198.C-0836(A).
⋆⋆ Visiting Astronomer, Complejo Astronómico El Leoncito operated under agreement between the Consejo Nacional de Investigaciones Científicas y Técnicas de la República Argentina, the National Universities of La Plata, Córdoba, San Juan.

spectra, which are occasionally complemented with CASLEO observations. Some recent findings of our new programme can be found in Flores et al. (2016, 2017, 2018).

Our sample includes the star HD 38858 (=HIP 27435). This nearby object is located at ∼15 pc (Gaia Collaboration 2016), presents a $B - V$ colour of 0.64 (Ducati 2002), and is of spectral type G2 V (Gray et al. 2003). In addition, the following atmospheric parameters have been reported: $T_{\rm eff}$ = 5733 ± 12 K, $\log g$ = 4.51 ± 0.01, [Fe/H] ∼ –0.22 ± 0.01, and $v_{\rm turb}$ = 0.94 ± 0.02 km s$^{-1}$ (Delgado Mena et al. 2017). Although the low metallicity value of HD 38858 ([Fe/H] ∼ –0.22 ± 0.01) would exclude it from some solar-analogue star definitions (e.g. Ramírez et al. 2010), it is considered, even following different criteria, as a solar-analogue star by several literature works (e.g. Hall et al. 2009; González Hernández et al. 2010; Delgado Mena et al. 2014). In addition, it is important to point out that the top ten of solar analogues from Soubiran & Triaud (2004) are composed of stars with metallicities in the range of –0.23 to +0.11 dex.

The HARPS monitoring of this star currently provides a large data set, enough for a detailed long-term stellar activity study of HD 38858. Moreover, due to the solar-analogue nature of this star, it could be used for a direct comparison with our Sun. In this way, HD 38858 constitutes an excellent laboratory for performing a comparative study of their chromospheric patterns (e.g. mean activity level, cycle length, and cycle amplitude), which has been done for only a few stars, such as 18 Sco (Hall et al. 2007) and HD 45184 (Flores et al. 2016).

For the solar case, Livingston & Holweger (1982) first revealed the spectral variation of several Fraunhofer lines along its ∼11 yr activity cycle (which is well tracked by the Ca II H&K lines). Subsequently, Livingston et al. (2007) reported that the Fe lines did not show the modulation expected with the Ca II H&K lines. For the stellar case, the possible cyclic modulation between Ca II H&K with both H$\alpha$ and metallic-line variations is poorly known. Gomes da Silva et al. (2014) studied the correlation between the flux of Ca II H&K and H$\alpha$ lines (through the $I_{\rm H\alpha}$ index) in an stellar sample of 271 FGK stars, finding that 23% out of 271 stars are correlated. In particular, the solar analogue star HD 45184 is included in the group of stars that do not show a correlation between these fluxes. However, we detected variations in the Balmer and Fe lines in this star (Flores et al. 2016), modulated by its ∼5.1 yr chromospheric activity cycle. The behaviour of the lines in this object is different to that observed in the Sun, in spite of their similar stellar parameters. Another solar-analogue star that does not show correlation is HD 38858 (see Table B.2. of Gomes da Silva et al. 2014). Then, similar to the case of HD 45184, studying the variability of the H$\alpha$ line in HD 38858 can be used to test the Ca II H&K–$I_{\rm H\alpha}$ correlation. These puzzling patterns show that long-term activity studies of stars similar to our Sun are necessary for a complete understanding of the observed phenomena.

The two main techniques for the detection of extrasolar planets, that is, transits and radial velocities (RVs), can be affected by stellar activity (e.g. Santos 2008; Martínez-Arnáiz 2011). In particular, RVs could vary due to the presence of active regions, which hinder the convection pattern (Campbell et al. 1988; Dravins 1985, 1992) and give place to a correlation between stellar activity and RV (e.g. Dravins 1992; Gomes da Silva et al. 2012; Dumusque et al. 2011). In this way, an activity cycle could introduce a periodic signal into the RV, which can be easily confused with the signal of an exoplanet (e.g. Martínez-Arnáiz et al. 2010; Dumusque et al. 2011; Gomes da Silva et al. 2012; Carolo et al. 2014). Mayor et al. (2011) announced the discovery of a radial super-Earth planet (minimum mass of 30.55 $M_\oplus$) orbiting HD 38858 with a period of 407.15 d, although this detection was not confirmed later. Recently, using a more extensive data set, Kennedy et al. (2015) pointed out that the signal associated with this supposed planet is an alias of a stellar activity cycle (with a period of 2930 d). However, through these additional data, the authors found another planetary signal with a period of 198 ± 1 d (0.64 AU) and minimum mass of 12 ± 2 $M_\oplus$. Nevertheless, it should be stressed that the corresponding analysis has not been published yet.

Although stellar activity can be a source of noise in precise RV measurements, it can be corrected for if activity is simultaneously measured using indexes, such as the Ca II H&K and H$\alpha$ lines. This shows that the study of the activity proxies and their relation with the RV is crucial to diminish the activity effects on RV measurements (Martínez-Arnáiz et al. 2010; Lovis et al. 2011; Gomes da Silva et al. 2014). In other words, it could provide valuable information for distinguishing between stellar and planetary signals. Fortunately, the long-term data base for the solar-analogue star HD 38858 allows us to carry out this type of study.

This work is organized as follows. In Sect. 2 we describe the observations and data reduction, in Sect. 3 we describe our analysis of chromospheric activity, and in Sect. 4 we present our discussion and conclusions.

## 2. Observations and data reduction

Our study is based on spectra of HD 38858 that we downloaded from the European Southern Observatory (ESO) archive[1] (Mayor et al. 2003). The spectra were acquired with the HARPS spectrograph, attached to the La Silla 3.6 m (ESO) telescope. This spectrograph is fed by a pair of fibres with an aperture of 1 arcsec on the sky, resulting in a resolving power of ∼115 000[2]. The observations were taken between 2003 and 2017 and have been automatically processed by the HARPS pipeline[3], covering a spectral range between 3782 and 6913 Å. After discarding a few observations with a low signal-to-noise ratio (S/N), we obtained a total of 237 spectra with an S/N ranging from 100 to 350 at 6075 Å. Then, these spectra were normalised and cleaned from cosmic rays and telluric features using IRAF[4] routines, as in our previous work (Flores et al. 2016).

We complement our analysis with observations obtained at the Complejo Astronómico El Leoncito (CASLEO, San Juan, Argentina). These observations, taken between 2012 and 2014, were acquired with the REOSC spectrograph mounted at the 2.15 m telescope. These medium-resolution echelle spectra ($R$ ∼ 13 000) range from 3890 to 6690 Å and were reduced using standard IRAF routines.

In order to compute the standard Mount Wilson index ($S_{\rm MW}$), we integrated the flux in two windows centred at the cores of the Ca lines, weighted with triangular profiles of a 1.09 Å

[1] http://archive.eso.org/wdb/wdb/adp/phase3_spectral/form?phase3_collection=HARPS
[2] http://www.eso.org/sci/facilities/lasilla/instruments/harps/overview.html
[3] http://www.eso.org/sci/facilities/lasilla/instruments/harps/doc.html
[4] IRAF is distributed by the National Optical Astronomical Observatories, which is operated by the Association of Universities for Research in Astronomy, Inc., under a cooperative agreement with the National Science Foundation.

full width at half-maximum (FWHM), and computed the ratio of these fluxes to the mean continuum flux, integrated in two passbands of 20 Å width centred at 3891 and 4001 Å. Finally, the $S_{\rm MW}$ indexes from both HARPS and CASLEO spectra were obtained using the calibration procedures explained in Lovis et al. (2011) and Cincunegui et al. (2007), respectively (see Flores et al. 2017, for details).

## 3. Activity cycle

### 3.1. Chromospheric emission at Ca II H&K lines

In Fig. 1 (upper panel) we show the time series of the $S_{\rm MW}$ for HD 38858. Here, we included all data, that is, HARPS and CASLEO observations and the corresponding monthly average values. These averaged data allow us to remove short-timescale variations caused by the transit of individual active regions (spots and plages). This same procedure has been applied in previous works (e.g. Baliunas et al. 1995; Metcalfe et al. 2010; Flores et al. 2018). The error bars of HARPS data correspond to the standard deviation of the mean. For bins with only one measurement, we adopted the typical dispersion of other bins. Then, we derived a long-term activity period of $3940 \pm 290$ d (~10.8 yr) by applying the generalised Lomb-Scargle periodogram (thereafter GLS, Zechmeister & Kürster 2009) to the seasonal means (Fig. 2). The false-alarm probability (thereafter FAP) of the main resulting period of $3.23 \times 10^{-13}$ was calculated following Zechmeister & Kürster (2009; see their Eq. (24) for details). Together with the more significant peak, two additional, less significant peaks are visible at $\sim 425 \pm 8$ d (FAP $\sim 3.08 \times 10^{-2}$) and $\sim 336 \pm 6$ d (FAP $\sim 1.65 \times 10^{-2}$). However, because we adopted a cut-off in FAP of 0.1 per cent (0.001) for reliable periodicities, neither period (likely aliases of the long-term cycle) was taken into account. We stress that according to Baliunas et al. (1995), our period FAP $\sim 3.23 \times 10^{-13}$ would be classified as excellent (FAP $\leq \times 10^{-9}$).

It is important to mention that HD 38858 not only has an activity cycle similar to that of our Sun (~11 yr), but its mean chromospheric activity level $\log(R'_{\rm HK}) = -4.94$ is also very similar to the solar values published by Hall et al. (2007) and Mamajek & Hillenbrand (2008) (–4.94 and –4.91, respectively). This activity index is obtained after subtracting the photospheric contribution, according to the Noyes et al. (1984) calibration. It is also worth mentioning that according to Baliunas et al. (1995), HD 38858 is simultaneously a nearly flat star ($\sigma_S/\overline{S} \approx 1.5\%-2\%$) and a cycling one (FAP $\leq 10^{-2}$). Furthermore, in Fig. 1, we observe that the $S_{\rm MW}$-cycle shape is similar to the sunspot cycles (Hathaway et al. 1994). It presents a sudden rise toward its maximum and a slower decay to the minimum. Du (2011) proposed a modified Gaussian distribution to fit and predict the solar cycles. This formula was recently corrected by Egeland et al. (2017) with an offset to the expression:

$$f = A \exp\left(-\frac{(t - t_{\rm m})^2}{2B^2[1 + \alpha(t - t_{\rm m})]^2}\right) + f_{\rm min}, \quad (1)$$

where $A$ represents the maximum value, $t_{\rm m}$ the time when the cycle reaches maximum if $t$ is computed from the minimum, $B$ is the width of Gaussian curve, and $\alpha$ is an assymetry factor. Although Eq. (1) can successfully model several solar cycles, it cannot reproduce the double peaks present in recent cycles.

In particular, Egeland et al. (2017) applied this formula to fit the Mount Wilson indexes obtained for the Sun during its Cycle 23. Following the numerical method described in this work, we

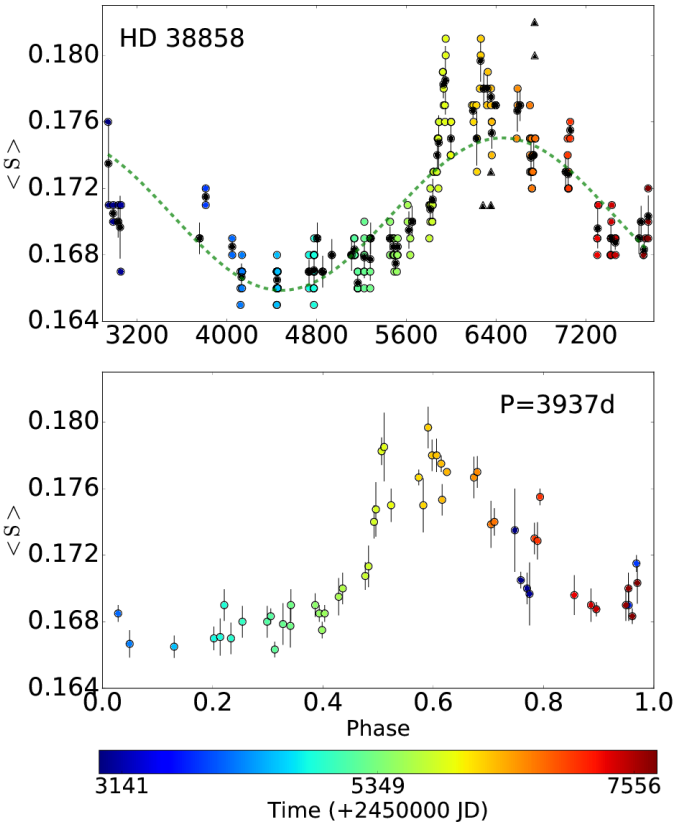


**Fig. 1.** *Upper panel*: individual $S_{\rm MW}$ measurements (coloured circles) and seasonal means (black full circles) from HARPS observations. The black triangles correspond to CASLEO data. The dotted green line shows a harmonic curve with the cycle calculated in this work. *Lower panel*: Mt Wilson index phased with a 10.8 yr period.

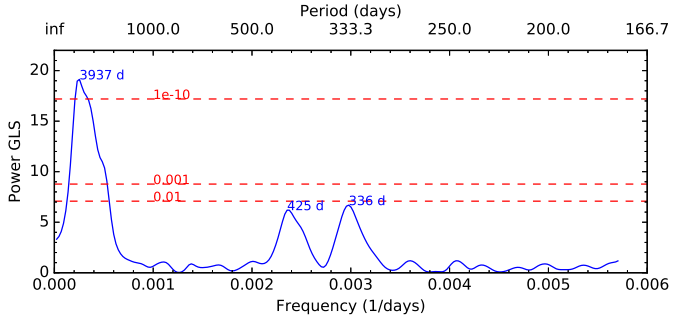


**Fig. 2.** GLS periodogram for the Mount Wilson indexes data plotted in Fig. 1 (*upper panel*).

fit Eq. (1) to the HD 38858 stellar cycle and obtained the parameters listed in Table 1 with a Pearson correlation coefficient of 0.90.

In Fig. 3 we show the mean Mount Wilson series and the corresponding cycle fit obtained for HD 38858 together with the cycle derived by Egeland et al. (2017) for solar cycle 23. Thus, if we compare the obtained parameters for the fitted stellar cycle with the solar parameters ($A_\odot = 0.0150$, $B_\odot = 2.154$ and $\alpha_\odot = 0.0343$), we observe that they are slightly different. However, the shape proposed in Eq. (1) successfully fits the stellar cycle.

The star HD 38858 has an activity period of $\sim 10.8 \pm 0.8$ yr. The period of the solar activity cycle ranges between 9 and 13 yr, with an average of 11 yr and a standard deviation of about 1.16 yr

**Table 1.** Fit parameters from Eq. (1) for HD 38858.

| Parameter | Value |
|---|---|
| $A$ | $0.0101 \pm 0.0001$ |
| $B$ | $1.44 \pm 0.04$ yr |
| $\alpha$ | $0.1052 \pm 0.019$ yr$^{-2}$ |
| $t_m$ | $2013.018 \pm 0.063$ |
| $f_{min}$ | $0.16709 \pm 0.0002$ |

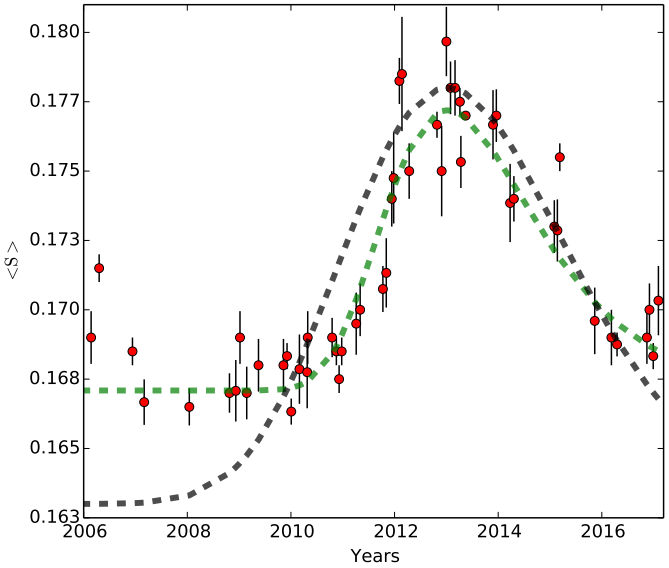


**Fig. 3.** Time series of the Mt Wilson indexes for HD 38858 (full red circles). The dashed green line corresponds to the fitted cycle, while the dashed grey line corresponds to the cycle derived for solar cycle 23.

(Hathaway 2010). Then, it is difficult to know whether the metallicity difference of 0.22 dex of the two stars plays a role in the length of the periods. Up to now, there is no clear observational evidence for the relation between cycle period and metallicity. For instance, Brandenburg et al. (2017) analysed the cycle periods of 35 FGK stars and did not find a clear relation with metallicity. Thus, studying a larger sample of solar-analogue and solar-twin stars with measured activity cycles and metallicities very different to that of the Sun could help to clarify this issue.

### 3.2. Activity-mimicking case, or a super-Earth planet orbiting HD 38858?

In Fig. 4 we plot the time series of the RV measurements for all HARPS spectra. A first glance at this figure reveals a clear modulation that also seems very similar to the activity modulation (see Fig. 1). As we described previously, this RV variation might be produced by stellar activity and not by an extrasolar planet. To test this possibility, we calculated the GLS periodogram for these data (Fig. 5). As a result, we detect a significant period of $\sim 3100 \pm 200$ d with a FAP of $6.47 \times 10^{-14}$ and two short less significant periods of $\sim 420 \pm 4$ d (FAP $\sim 1.28 \times 10^{-6}$) and $\sim 326 \pm 8$ d (FAP $\sim 3.24 \times 10^{-1}$), respectively. We note that these three peaks are close to the values obtained from the stellar activity analysis (see Fig. 2). Then, in order to rule out possible alias peaks of the long-term signal (i.e. $\sim 3100$ d), we subtracted it and recalculated the corresponding GLS periodogram, according to Suárez Mascareño et al. (2016)

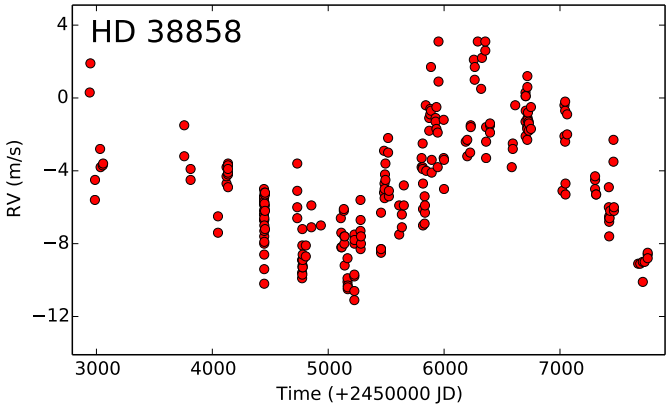


**Fig. 4.** Time series of RV measurements obtained from HARPS spectra.

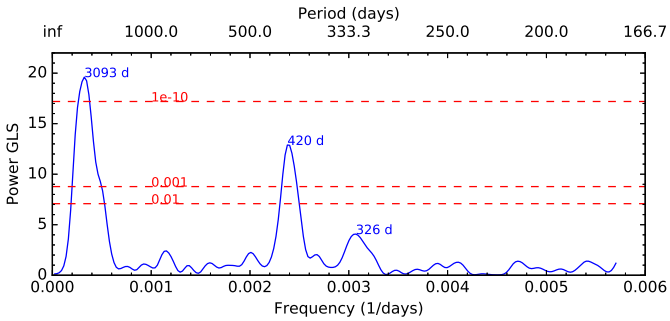


**Fig. 5.** GLS periodogram for the RVs plotted in Fig. 4.

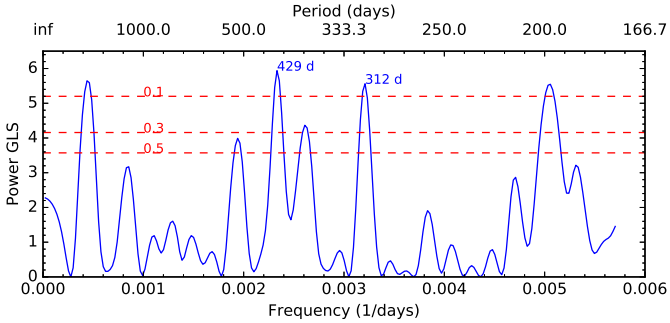


**Fig. 6.** GLS periodogram after subtracting the ~3100 d period.

and Flores et al. (2018). As a result, Fig. 6 shows that the two less significant periods are now absent, which indicates that these peaks correspond to aliases.

In addition, in Fig. 7 we plot the RV versus $\log(R'_{HK})$. We applied a Bayesian analysis to these data to asses the presence of a possible correlation. Using the *python* code provided by Figueira et al. (2016), we estimated the posterior probability distribution of the correlation coefficient $\rho$. From this test, we obtained a correlation coefficient of $0.744 \pm 0.029$ with a 95% credible interval between 0.688 and 0.800. Thus, the similarity between the time series together with the GLS periodogram analysis and also the RV–$\log(R'_{HK})$ trend suggest that the signal attributed to HD 38858b could be related to stellar activity and probably not to a super-Earth, as claimed by Mayor et al. (2011) and considered in subsequent statistical works (e.g. Delgado Mena et al. 2014; da Silva et al. 2015; Mishenina et al. 2016). This conclusion was first reached by Kennedy et al. (2015). However, until now, the corresponding analysis that supports this claim has not been published.

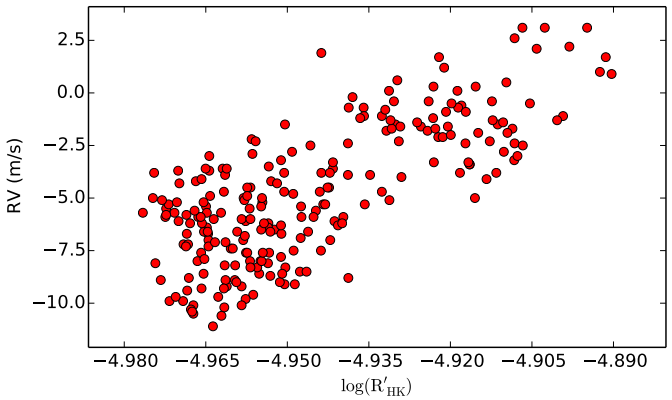


**Fig. 7.** RV vs. $\log(R'_{\rm HK})$ for HD 38858.

### 3.3. Searching for variations in the Balmer and metallic lines

We applied different techniques to search for small spectral variations in hydrogen and metallic lines throughout the activity cycle. As a prior step, we made a general evalution of noise in our spectroscopic material in order to estimate the level above which possible variations can be considered reliable. This was motivated by the detection of non-random modulations in residual spectra (individual minus average), which might impose a minimum threshold for long-term variability detection. The shape of these systematic patterns suggests that they are related to normalization, echelle-order tracing, order merging, and wavelength calibration problems.

In order to estimate the typical noise level, we calculated the RMS of residual spectra using small spectral windows without strong spectral lines. The obtained values are typically in the range 0.003–0.008, in units of the continuum level. To evaluate the presence of non-random noise, we convolved the residual spectra with boxy kernels of increasing size ($n$ pixels) and analysed the behaviour of the RMS as a function of $n$. Pixel-to-pixel random noise is expected to decrease as $n^{-1/2}$, while low-frequency noise is not damped until wide enough kernels are used. In this way, by modelling the observed function RMS($n$) with an $n^{-1/2}$ term plus a low-frequency component, we obtained rough estimates of the contribution of non-random noise.

Typically, random noise (mainly photon noise) is 0.6% of the continuum level, while non–random errors on scales similar to spectral features (10–40 pixels) are of the order of 0.1%. In addition, run–to–run low–frequency modulations (normalisation) of the order 0.5% are present, but they are easily filtered without altering most spectral features. In summary, in a typical individual spectrum, our detection limit for variations is about 0.6%, which for most spectral lines, whose profiles cover 10–40 pixels, corresponds to equivalent width ($W_{\rm eq}$) variations of 0.2–0.4 mÅ[5]. At this level there are no evident spectral variations other than the resonance doublet lines of Ca II. On the other hand, even though many spectra of the same run can be combined to improve the S/N ratio, we considered the flux uncertainty to be always at least 0.1% on the continuum level.

As a first strategy to search for intensity variation of metallic lines, we calculated the $W_{\rm eq}$ of the line profiles for several strong Fe II lines. Figure 8 shows the $W_{\rm eq}$ variations of the Fe II line at 5018 Å. The point distribution suggests an increase of this Fe II line with stellar activity. The period detection from these data using the GLS periodogram (see Fig. 9) should be considered as marginal (FAP $\sim 1.6\times10^{-3}$), according to our fixed cut-off. Thus, the activity cycle is not easily detected in these lines.

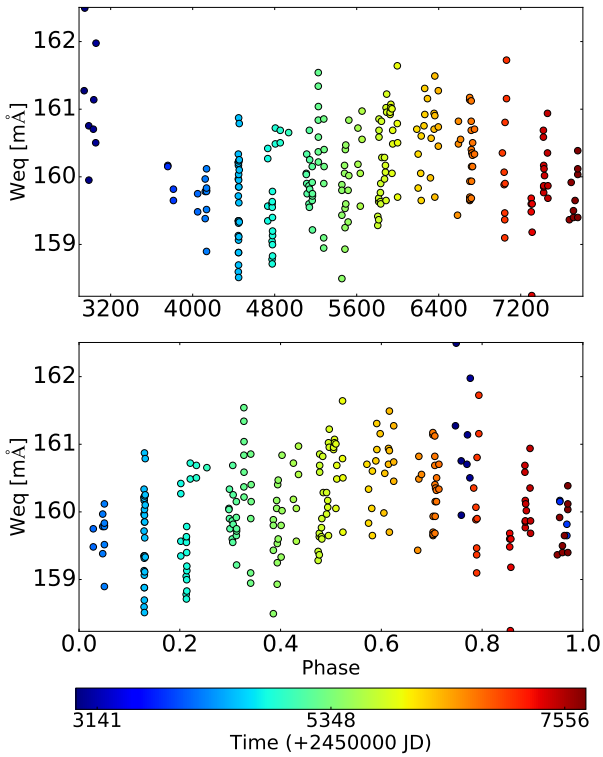


**Fig. 8.** *Upper panel*: $W_{\rm eq}$ variation of the Fe II 5018 Å line. *Lower panel*: $W_{\rm eq}$ phased with a 10.8 yr period.

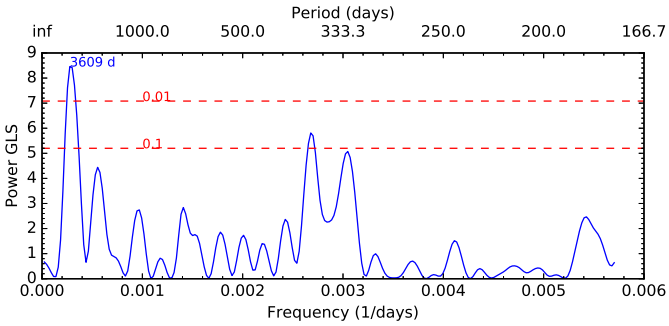


**Fig. 9.** GLS periodogram of the $W_{\rm eq}$ data plotted in Fig. 8.

With the aim to detect low-level spectral variations related specifically to the timescale of the activity cycle, we applied two strategies. On the one hand, we calculated two mean spectra at low and high activity. The high-activity spectrum was calculated by averaging the 42 spectra taken between December 2011 and February 2014 (HJD 2455926–2456705), while the low-activity spectrum was the average of 91 spectra obtained between November 2006 and March 2010 (HJD 2454049–2455283). Then, we calculated the difference between them and searched for significant features in the difference spectrum. Random errors in these mean spectra are expected to be reduced to about 0.09% and 0.06%, respectively. Thus considering that spectral features are about 10–20 pixels wide, false variability features of 0.03% are expected to be present due to random noise. This value is lower than the non-random errors mentioned above, which might reach ~0.1%. We therefore considered

[5] For weak lines the uncertainty in $W_{\rm eq}$ is $\sigma_{\rm Weq} = n^{1/2}\cdot\Delta\cdot(S/N)^{-1}$, where $\Delta$ is the pixel size in wavelength units, and $n$ is the integration aperture in pixels.

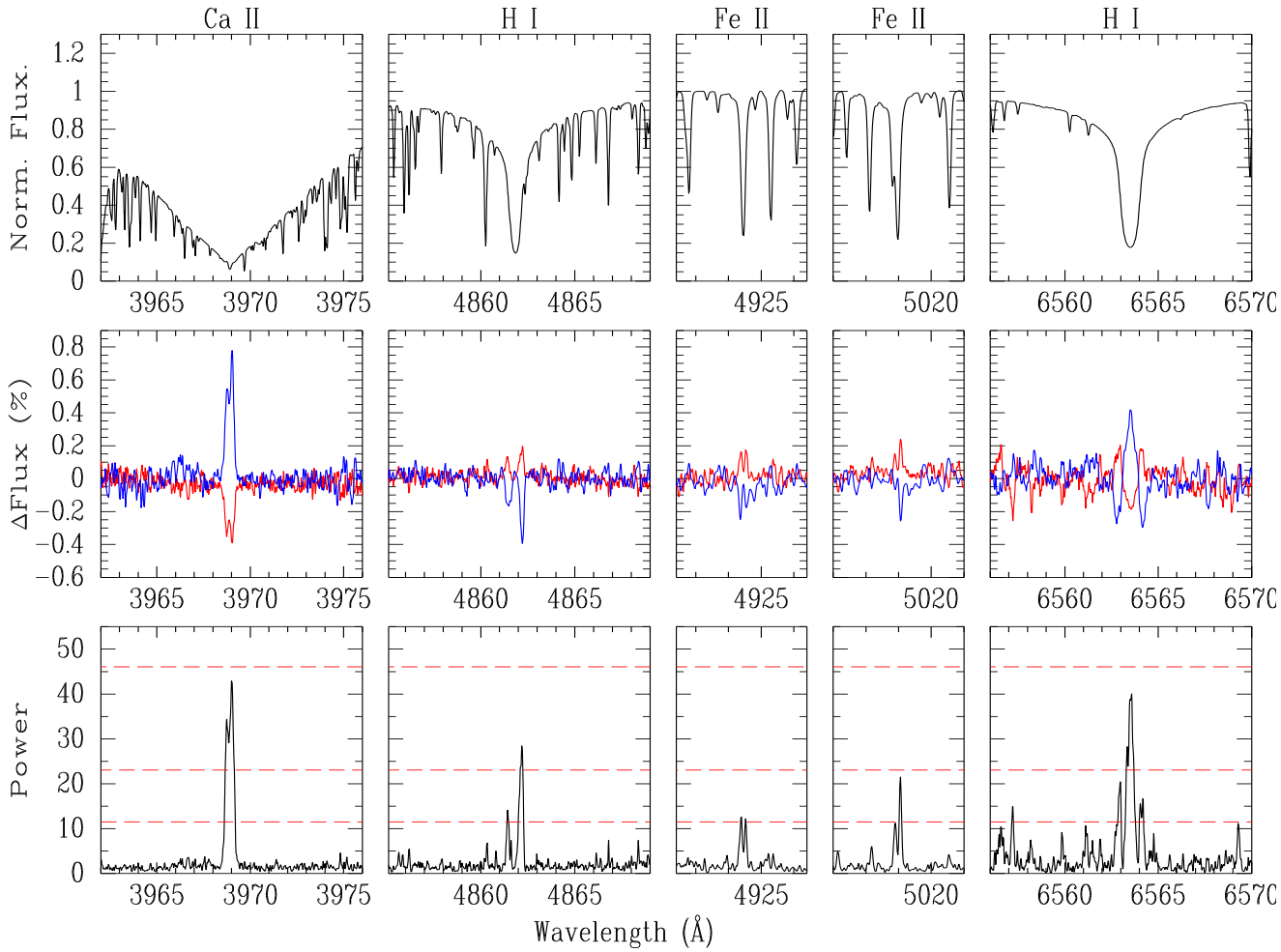


**Fig. 10.** Spectral variation of optical lines. *Upper panel*: mean spectra near the lines Ca II H, H$\beta$, Fe II 4924 Å, Fe II 5018 Å, and H$\alpha$. *Middle panel*: differences between the high-activity (blue line) mean spectrum and the mean reference spectrum and the low-activity (red solid line) mean spectrum and the mean reference spectrum. *Lower panel*: periodogram height at $P$ = 3940 d for each spectrum pixel. Horizontal dashed lines correspond to FAP = $10^{-5}$, $10^{-10}$, and $10^{-15}$ (see text for explanation).

spectral lines to be variable if there is a difference of at least 0.2% between the epochs of low and high activity.

Figure 10 shows the difference between the high-activity (low-activity) mean spectrum and the mean reference spectrum around five spectral lines: $\lambda$3968 Ca II, H$\alpha$, H$\beta$, and two strong iron lines that were reported to be sensitive to chromospheric activity in HD 45184. Clear variations are seen in the core of H I lines. In the position of the Fe II lines, there would be small differences between low- and high-activity spectra, although they should be considered as marginal detections, since they are close to 0.2%. This is consistent with results obtained from equivalent widths.

On the other hand, from the spectral time-series we extracted the light curve corresponding to each wavelength and calculated the power of the periodogram for the adopted value for the activity period. This is shown in the lower panels of Fig. 10. The Balmer lines appear to be clearly variable with an FAP in the range $10^{-10}$–$10^{-20}$ , while iron lines present an FAP somewhat lower but still higher than $10^{-5}$. Our aim is to detect spectral features that vary with the activity cycle, therefore these FAP calculations correspond to a fixed period given a priori, and not to the maximum peak for a grid of frequencies.

In addition to the Ca II lines, the most clearly variable line is H$\alpha$. The variations cover about 2–3 Å around the core of the line, making the detection highly reliable. The variation mainly affects the shape of the line profile, without significant variations in $W_{\rm eq}$, since the flux variations at the very centre of the line is opposite to that at about 0.7 Å from the line centre. These profile variations are not detected by techniques that are based on flux integration in a given window. To show this, we plot in Fig. 11 the time series for the $W_{\rm eq}$ of H$\alpha$ line, while the corresponding GLS periodogram is shown in Fig. 12. There is no significant periodic signal in the equivalent width time series.

A similar behaviour was found in HD 45184, where we used the kurtosis of the line core to analyse the variability. We adopted a different strategy here. To use the shape of H$\alpha$ as activity proxy, we made a mask representing the activity effects on the profile of H$\alpha$. Specifically, we calculated the difference between the high- and low-activity spectra and applied a smoothing by convolving the profile with a Gaussian of width $\sigma$ = 0.2 Å and apodised the edges by multiplying by a cosine with full intensity in the central 1.5 Å and zero out of a window of 5.0 Å (See Fig. 13).

We define an activity index $I_\alpha$ as the integral of the product of this mask $M$ with the observed spectrum $S$:

$$I_\alpha = \int S(\lambda) \cdot M(\lambda)\, {\rm d}\lambda, \qquad (2)$$

where $M = H - L$, being $H$ the high-activity mean spectrum and $L$ the low-activity mean spectrum. We note that $I_\alpha$ is positive when the spectrum $S$ is more similar to $H$ than to $L$ and vice

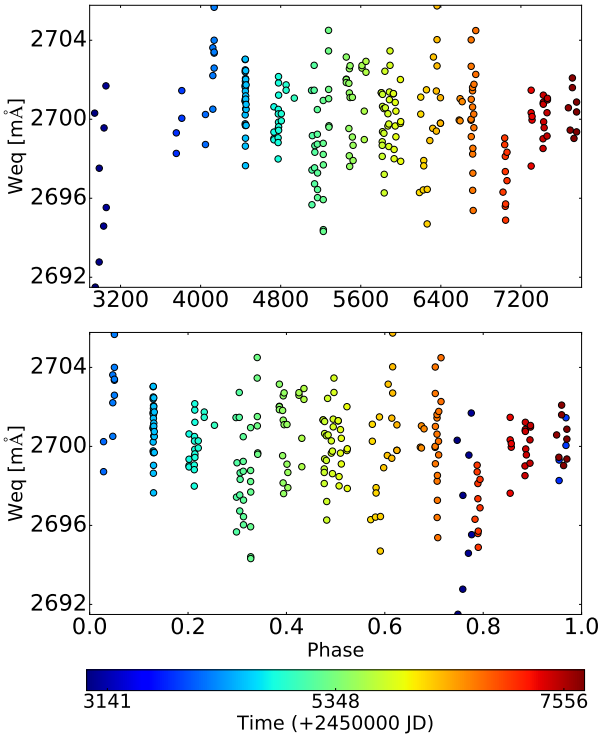


**Fig. 11.** *Upper panel*: $W_{eq}$ variation of H$\alpha$ Å line. *Lower panel*: $W_{eq}$ phased with a 10.8 yr period.

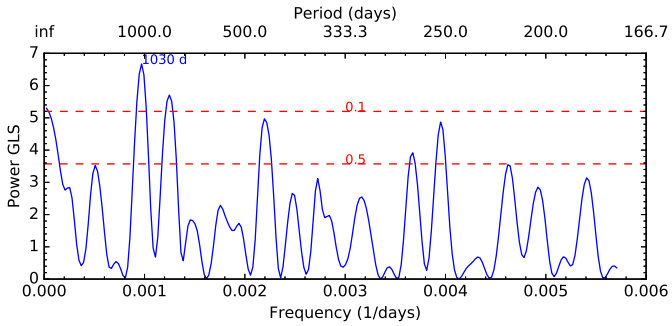


**Fig. 12.** GLS periodogram of the $W_{eq}$ data plotted in Fig. 11.

versa:

$$I_\alpha = \int (S - L)^2 \, \mathrm{d}\lambda - \int (S - H)^2 \, \mathrm{d}\lambda + \text{const.} \quad (3)$$

We measured the activity parameter $I_\alpha$ in all HARPS spectra of HD 38858 and obtained the results shown in Fig. 14 (upper panel). The spectral variations clearly replicate the behaviour of the Mt Wilson activity index. In an attempt to verify the period of the activity cycle, in Fig. 14 (lower panel) we also show the $I_\alpha$ parameter phased with the chromospheric ~10.8 yr activity period. The good agreement between the Ca II and $I_\alpha$ variations is clear (see Fig. 1 for comparison).

## 4. Discussion and conclusions

We performed a detailed study of stellar activity in the solar analogue HD 38858, which shows several spectral lines with signs of appreciable variations. To do so, we have analysed a total of 242 HARPS and CASLEO spectra. As a result, we found a chromospheric activity cycle of ~10.8 yr with an amplitude

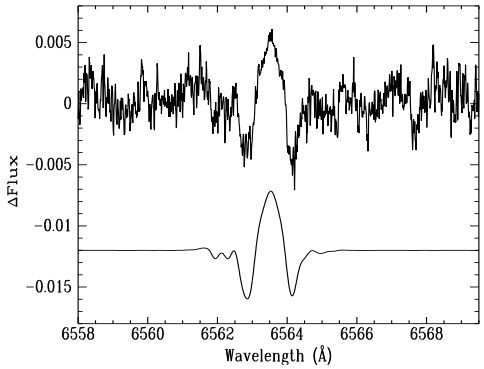


**Fig. 13.** Difference between the high- and low-activity mean spectra (*up*) and the corresponding H$\alpha$ mask (*bottom*) used to analyse the spectral variations. The flux is normalised to the original continuum level; the lower spectrum has been shifted for better visibility.

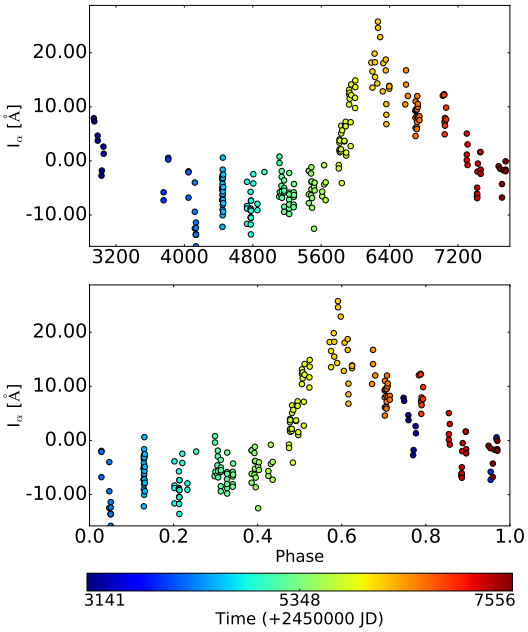


**Fig. 14.** *Upper panel*: time series of the $I_\alpha$ activity parameter. *Lower panel*: $I_\alpha$ variation phased with a ~10.8 yr period.

$\Delta S \sim 0.013$, a mean $S_{MW}$ index of 0.170 ($\log(R'_{HK}) = -4.94$), and a shape of the stellar cycle that is similar to that of the Sun. Although the solar cycle fluctuates in amplitude, shape, and length (Charbonneau 2010; Hathaway 2010), the corresponding values obtained for HD 38858 indicate that its activity behaviour could be similar to the Sun.

On the other hand, the GLS periodogram of HARPS radial velocities reveals two significant peaks. One of them corresponds to the long-term chromospheric activity cycle, which is produced by the active regions situated in the chromosphere of the star. The second peak of $420 \pm 4$ d is an alias of the more significant peak, which was initially interpreted as the signal of a super-Earth planet by Mayor et al. (2011). However, our analysis clearly shows that this radial velocity modulation is produced by stellar activity, in agreement with the previous claim of Kennedy et al. (2015).

It is believed that there is no a simple relation between different activity proxies. For instance, for the case of the Ca II H&K and H$\alpha$ line correlation in solar-type stars, some authors attribute the discrepancies to the activity level and metallicity

(Gomes da Silva et al. 2014), while others suggest that this correlation is complex and depends on the star under consideration (Cincunegui et al. 2007). In addition, Flores et al. (2016) recently found in HD 45184, a star with physical properties similar to those of HD 38858, that the statistical moments, including the $W_{eq}$ of the Balmer and some Fe II lines (4924 Å, 5018 Å, and 5169 Å), are modulated by the chromospheric cycle. The existence of another activity proxy different from the Ca II H&K lines is important not only as a tool for searching activity cycles, but also to distinguish planetary from stellar signals in the planet-search RV surveys that do not include the Ca II H&K lines. Here, the Ca II H&K modulation (chromospheric cycle) of HD 38858 is also evident in the Balmer lines (H$\alpha$ and H$\beta$), while Fe II at 4924 Å and 5018 Å result in marginal detections.

Gomes da Silva et al. (2014) analysed the possible correlation between $\log(R'_{HK})$ and $\log(I_{H\alpha})$[6] in a stellar sample of 271 FGK stars through the Pearson correlation coefficient. As a result, only 23% of these stars were correlated (20% showed a positive and 3% a negative correlation). Notably, they included HD 38858 in the group of stars that did not show any correlation, with a high level of significance. We here detected in HD 38858 spectral variations that affect the shape of the H$\alpha$ core, and demonstrated that these variations are correlated with the activity index $\log(R'_{HK})$. This finding substantiates our previous results obtained for HD 45184, another star without a H$\alpha$–$\log(R'_{HK})$ correlation, according to Gomes da Silva et al. (2014), for which we had detected variations in the H$\alpha$ profile through the analysis of the kurtosis of the line core. Therefore, our results suggest that at least in solar-analogue stars, the shape of the H$\alpha$ line profile would be a better candidate than the net flux when we wish to search for correlations with stellar activity.

This has relevance for the definition of alternative activity proxies. Gomes da Silva et al. (2014) also demonstrated that the flux at the H$\alpha$ core is not a sensitive indicator for detecting magnetic cycles. In a sample of 271 stars, they were able to find activity cycles in 26% using the $\log(R'_{HK})$ index, but when they used their $I_{H\alpha}$ index, they found cycles in only 3%. However, we detected chromospheric cycles in the stars HD 45184 and HD 38858 (with periods of 5.14 and 10.8 yr, respectively) by studying the H$\alpha$ variations. Then, both HD 45184 and HD 38858 are remarkable objects, showing clear cycles detected in $\log(R'_{HK})$ and also in the H$\alpha$ profile, with a supposed null $I_{H\alpha}$ correlation (Gomes da Silva et al. 2014).

At the current state of knowledge, gathering observational data is crucial. The only way to shed light on these issues is to perform detailed spectral analyses of the different activity proxies in a wide sample of solar-type stars. For this reason, we are currently starting to search for Fe II line variations and study the Ca II H&K and H$\alpha$ correlation in a significant star sample using available HARPS data.

*Acknowledgements.* We warmly thank the anonymous referee for the careful reading of the manuscript and constructive comments that enabled the work to be improved. M. F., M. J and F. M. L. also acknowledge the financial support from CONICET in the forms of post-doctoral fellowships.

## References

Baliunas, S. L., Donahue, R. A., Soon, W. H., et al. 1995, ApJ, 438, 269
Brandenburg, A., Mathur, S., & Metcalfe, T. S. 2017, ApJ, 845, 79
Campbell, B., Walker, G. A. H., & Yang, S. 1988, ApJ, 331, 902
Carolo, E., Desidera, S., Gratton, R., et al. 2014, A&A, 567, A48
Charbonneau, P. 2010, Living Rev. Sol. Phys., 7, 3
Cincunegui, C., Díaz, R., & Mauas, P. 2007, A&A, 469, 309
da Silva, R., Milone, A. D. C., & Rocha-Pinto, H. J. 2015, A&A, 580, A24
Delgado Mena, E., Israelian, G., González Hernández, J. I., et al. 2014, A&A, 562, A92
Delgado Mena, E., Tsantaki, M., Adibekyan, V. Z., et al. 2017, A&A, 606, A94
Donahue, R. A. 1993, PhD Thesis, New Mexico State University, University Park
Dravins, D. 1985, in Stellar Radial Velocities, eds. A. G. D. Philip, & D. W. Latham, 88, 311
Dravins, D. 1992, in European Southern Observatory Conference and Workshop Proceedings, ed. M.-H. Ulrich, 40, 55
Du, Z. 2011, Sol. Phys., 273, 231
Ducati, J. R. 2002, VizieR Online Data Catalog: II/237
Dumusque, X., Lovis, C., Ségransan, D., et al. 2011, A&A, 535, A55
Duncan, D. K., Vaughan, A. H., Wilson, O. C., et al. 1991, ApJS, 76, 383
Egeland, R., Metcalfe, T. S., Hall, J. C., & Henry, G. W. 2015, ApJ, 812, 12
Egeland, R., Soon, W., Baliunas, S., et al. 2017, ApJ, 835, 25
Figueira, P., Faria, J. P., Adibekyan, V. Z., Oshagh, M., & Santos, N. C. 2016, Origins Life Evol. Biosphere, 46, 385
Flores, M., González, J. F., Jaque Arancibia, M., Buccino, A., & Saffe, C. 2016, A&A, 589, A135
Flores, M. G., Buccino, A. P., Saffe, C. E., & Mauas, P. J. D. 2017, MNRAS, 464, 4299
Flores, M., Saffe, C., Buccino, A., et al. 2018, MNRAS, 476, 2751
Gaia Collaboration (Brown, A. G. A., et al.) 2016, A&A, 595, A2
Gomes da Silva, J., Santos, N. C., Bonfils, X., et al. 2012, A&A, 541, A9
Gomes da Silva, J., Santos, N. C., Boisse, I., Dumusque, X., & Lovis, C. 2014, A&A, 566, A66
González Hernández, J. I., Israelian, G., Santos, N. C., et al. 2010, ApJ, 720, 1592
Gray, R. O., Corbally, C. J., Garrison, R. F., McFadden, M. T., & Robinson, P. E. 2003, AJ, 126, 2048
Hall, J. C., Lockwood, G. W., & Skiff, B. A. 2007, AJ, 133, 862
Hall, J. C., Henry, G. W., & Lockwood, G. W. 2009, AJ, 138, 312
Hathaway, D. H. 2010, Living Rev. Sol. Phys., 7, 1
Hathaway, D. H., Wilson, R. M., & Reichmann, E. J. 1994, Sol. Phys., 151, 177
Henry, T. J., Soderblom, D. R., Donahue, R. A., & Baliunas, S. L. 1996, AJ, 111, 439
Kennedy, G. M., Matrà, L., Marmier, M., et al. 2015, MNRAS, 449, 3121
Livingston, W., & Holweger, H. 1982, ApJ, 252, 375
Livingston, W., Wallace, L., White, O. R., & Giampapa, M. S. 2007, ApJ, 657, 1137
Lovis, C., Dumusque, X., Santos, N. C., et al. 2011, ArXiv e-prints [arXiv:1107.5325]
Mamajek, E. E., & Hillenbrand, L. A. 2008, ApJ, 687, 1264
Martínez-Arnáiz, R., Maldonado, J., Montes, D., Eiroa, C., & Montesinos, B. 2010, A&A, 520, A79
Martínez-Arnáiz, R. M. 2011, PhD Thesis, Departamento de Astrofísica, Facultad de Ciencias Físicas, Universidad Complutense de Madrid, 28040 Madrid, Spain
Mayor, M., Marmier, M., Lovis, C., et al. 2011, A&A, submitted [arxiv:1109.2497]
Mayor, M., Pepe, F., Queloz, D., et al. 2003, The Messenger, 114, 20
Metcalfe, T., Basu, S., Henry, T. J., et al. 2010, ApJ, 723, L213
Mishenina, T., Kovtyukh, V., Soubiran, C., & Adibekyan, V. Z. 2016, MNRAS, 462, 1563
Nissen, P. E. 2015, A&A, 579, A52
Noyes, R. W., Hartmann, L. W., Baliunas, S. L., Duncan, D. K., & Vaughan, A. H. 1984, ApJ, 279, 763
Ramírez, I., Asplund, M., Baumann, P., Meléndez, J., & Bensby, T. 2010, A&A, 521, A33
Saffe, C., Flores, M., Jaque Arancibia, M., Buccino, A., & Jofré, E. 2016, A&A, 588, A81
Santos, N. C. 2008, New Astron. Rev., 52, 154
Skumanich, A. 1972, ApJ, 171, 565
Soubiran, C., & Triaud, A. 2004, A&A, 418, 1089
Suárez Mascareño, A., Rebolo, R., & González Hernández, J. I. 2016, A&A, 595, A12
Vaughan, A. H., Preston, G. W., & Wilson, O. C. 1978, PASP, 90, 267
Wilson, O. C. 1978, ApJ, 226, 379
Zechmeister, M., & Kürster, M. 2009, A&A, 496, 577

[6] This index measures the flux in the core of the H$\alpha$ line (see Gomes da Silva et al. 2014, for details).